EXPERIMENTAL EVIDENCE IN SUPPORT OF JOULE HEATING ASSOCIATED WITH GEOMAGNETIC ACTIVITY

by Leonard L. DeVries

George C. Marshall Space Flight Center
Marshall Space Flight Center, Ala. 35812

NATIONAL AERONAUTICS AND SPACE ADMINISTRATION • WASHINGTON, D. C. • NOVEMBER 1971

1. Report No.	2. Government Accession No.	3. Recipient
NASA TN D-6518		

4. Title and Subtitle	5. Report Date
Experimental Evidence in Support of Joule Heating Associated with Geomagnetic Activity	November 1971
	6. Performing Organization Code
7. Author(s)	8. Performing Organization Report No.
Leonard L. DeVries	M175
	10. Work Unit No.
9. Performing Organization Name and Address	976-30-00
George C. Marshall Space Flight Center Marshall Space Flight Center, Alabama 35812	11. Contract or Grant No.
	13. Type of Report and Period Covered
12. Sponsoring Agency Name and Address	Technical Note
National Aeronautics and Space Administration Washington, D.C. 20546	14. Sponsoring Agency Code

15. Supplementary Notes

Prepared by Aero-Astrodynamics Laboratory, Science and Engineering

16. Abstract

High resolution accelerometer measurements in the altitude region 140 to 300 km from a satellite in a near-polar orbit during a period of extremely high geomagnetic activity indicate that Joule heating is the primary source of energy for atmospheric heating associated with geomagnetic activity. This conclusion is supported by the following observational evidence: (1) There is an atmospheric response in the auroral zone which is nearly simultaneous with the onset of geomagnetic activity, with no significant response in the equatorial region until several hours later; (2) the maximum heating occurs at geographic locations near the maximum current of the auroral electrojet; and (3) there is evidence of atmospheric waves originating near the auroral zone at altitudes where Joule heating would be expected to occur. An analysis of atmospheric response time to this heat shows time delays are apparently independent of altitude but are strongly dependent upon geomagnetic latitude.

17. Key Words (Suggested by Author(s))	18. Distribution Statement
Earth Upper Atmosphere Joule Heating Atmospheric Density Variation Geomagnetic Storms	

19. Security Classif. (of this report)	20. Security Classif. (of this page)	21. No. of Pages	22. Price*
Unclassified	Unclassified	37	$3.00

*For sale by the National Technical Information Service, Springfield, Virginia 22151

TABLE OF CONTENTS

LIST OF ILLUSTRATIONS

LIST OF ILLUSTRATIONS (Concluded)

EXPERIMENTAL EVIDENCE IN SUPPORT OF JOULE HEATING ASSOCIATED WITH GEOMAGNETIC ACTIVITY

SUMMARY

High resolution accelerometer measurements in the altitude region 140 to 300 km from a satellite in a near-polar orbit during a period of extremely high geomagnetic activity indicate that Joule heating is the primary source of energy for atmospheric heating associated with geomagnetic activity. This conclusion is supported by the following observational evidence: (1) There is an atmospheric response in the auroral zone which is nearly simultaneous with the onset of geomagnetic activity, with no significant response in the equatorial region until several hours later; (2) the maximum heating occurs at geographic locations near the maximum current of the auroral electrojet; and (3) there is evidence of atmospheric waves originating near the auroral zone at altitudes where Joule heating would be expected to occur. An analysis of atmospheric response time to this heating shows time delays are apparently independent of altitude but are strongly dependent upon geomagnetic latitude.

INTRODUCTION

Variations in the density of the neutral atmosphere associated with geomagnetic activity were first discovered by Jacchia [1] during an investigation to establish an improved relationship between the solar radio flux at 10.7 cm and accelerations of satellites. He noted that the curve of the satellite accelerations agreed with the plot of the solar radio flux except for two transient, short-period secondary oscillations. These oscillations were coincident with the dates of the only two large geomagnetic disturbances that occurred during the lifetime of these particular satellites. Jacchia concluded from these results that corpuscular radiation capable of producing a large geomagnetic storm has a greater, although more transient, effect on atmospheric density at 200 km than the fluctuations in solar electromagnetic radiation associated with the 10.7-cm solar radio flux. Numerous analyses of high altitude density data during the past 10 years have shown that density increases are almost certain to occur simultaneously with, or shortly after, enhancement of geomagnetic activity.

POSSIBLE ATMOSPHERIC HEATING MECHANISMS

Several hypotheses have been proposed to explain the mechanism by which this heating occurs. Dessler [2] advanced the theory that such heating results from large amplitude waves that are formed on the edge of the earth's magnetosphere when it

interacts with the solar wind. He concluded that, although the electric conductivity of the ambient atmosphere at high altitudes is sufficiently high that dissipation of such waves due to electron-ion and ion-atom collisions is negligible, collisions between ions and neutral atoms at lower levels can cause a significant amount of heating. Dessler estimated that the altitude at which the maximum heating from hydromagnetic waves occurs was between 150 and 200 km. Akasofu [3] subsequently calculated the rise in atmospheric temperature due to the hydromagnetic waves which are likely to occur naturally in the expected frequency range (ω = 1-25 Hz) and found that it was not greater than 5 deg. These results indicate that hydromagnetic waves do not contribute significantly to atmospheric heating associated with geomagnetic activity.

Another possible mechanism explains heating of the ionosphere during magnetic disturbances as corpuscular bombardment by energetic charged particles. McIlwain [4] suggested that electrons in the energy range of 1 to 100 keV are absorbed primarily below 120 km altitude. Bremsstrahlung from these electrons would presumably be absorbed principally at lower altitudes. Cole [5] calculated an upper limit of energy put into the atmosphere by this mechanism of approximately 4×10^{-6} ergs cm^{-3} sec^{-1} and concluded that the amount of energy absorbed by neutral particles has little effect on their temperature because of the high density of the atmosphere below 120 km.

Cole [6] applied the results of earlier work by Cowling and Peddington [7] on Joule heating and motion of uniform ionized gas to the ionosphere during geomagnetic disturbances to explain the source of energy available during geomagnetic storms. Energetic particles participate into the auroral zones during periods of enhanced geomagnetic activity and provide some direct heat to the neutral thermosphere by conversion of their kinetic energy. In addition, the increase of electron density within the auroral zones results in an increase in electric currents within the ionospheric auroral electrojet and in associated heating of the thermosphere at high latitudes by Joule heating. Current of density (j) causes Joule heating at the rate Q given by j^2/σ_3, where σ_3 is the Cowling conductivity. Thus, since j is proportional to the magnetic disturbance, the power input is proportional to the electric current flowing in the ionosphere. Using the most likely estimates of j and σ, Cole computed energy sources associated with Joule heating. He concluded that they are more than sufficient to explain the heat balance of the disturbed ionosphere. Heating by this process occurs in the auroral zones almost simultaneously with the enhancement of geomagnetic activity at altitudes between 100 and 200 km. The heat transport to lower latitudes could be by heat conduction, heat convection, or wave mechanisms. The significant conclusions of this pioneering study by Cole [6] were:

1. Joule heating in the region 100 to 200 km altitude is common during geomagnetic disturbances.

2. Scale heights and temperatures at altitudes above about 100 km increase with geomagnetic disturbances.

3. Generally, the energy of the process causing a geomagnetic disturbance is not measurable by the energy of the geomagnetic disturbance.

4. A horizontal gradient of pressure at heights above 150 km is maintained in the auroral zone during geomagnetic disturbances.

5. Wind speeds in the polar ionosphere increase during geomagnetic disturbances.

OBSERVATIONAL EVIDENCE OF ATMOSPHERIC HEATING ASSOCIATED WITH GEOMAGNETIC ACTIVITY FROM STUDIES OF SATELLITE DECAY

Extensive studies of satellite drag-deduced density data [8] revealed several important details of density variations associated with geomagnetic activity. Some of these details are listed below.

1. Even small variations in geomagnetic activity are reflected in atmospheric density observations. The corresponding temperature variations appear related in a near-linear fashion with the planetary geomagnetic index, a_p, during magnetic storms proper; while during magnetically quiet periods, the relationship is nearly linear with the planetary index, K_p, which is the logarithmic counterpart of a_p. The empirical relationships between these quantities can be represented to a fair degree of accuracy by the relationship [8]

$$\Delta T = 1.0\, a_p + 100^\circ\, [1 - \exp(-0.08\, a_p)] \quad , \qquad (1)$$

where ΔT is the change in exospheric temperature.

2. Atmospheric perturbations lag behind geomagnetic perturbations by several hours, with an average time lag of 6.7 hours (7.2 hours at low altitudes, less than 6 hours at high latitudes).

3. The temperature during a geomagnetic disturbance is enhanced at high latitudes, at least occasionally.

It was recognized that transient density fluctuations such as those associated with geomagnetic activity are difficult to study by the satellite drag-analysis method because the time and spatial resolutions (about 5 hours or 3 orbits) are so large. Since the quantity to be determined, the acceleration of the satellite's mean motion, is the second derivative of the mean anomaly, this task becomes increasingly difficult. Another very important

limitation in the technique of deducing density values from satellite drag data is the fact that the change in the orbital period is a measure of the integrated effect of air drag in the neighborhood of perigee. This angular resolution is a function of the orbit eccentricity. For example, King-Hele [9] has calcualted that for an orbit with an eccentricity of 0.2 and a perigee altitude range of 200 to 250 km, the drag is appreciable over an arc of 20 deg on each side of perigee. Since this drag occurs at heights up to one scale height, H (about 25 km at altitudes of 200 to 250 km), above perigee, the resulting density value represents, assuming a time resolution of 0.2 day, an average through a region up to 25 km in height over a lateral geographic distance up to 3400 km. Thus, it is not surprising that analyses of these data lead to different conclusions concerning time delays of density increases following geomagnetic storms.

To identify the energy source and the mechanism by which the atmosphere is heated following geomagnetic storms, the intensity of the heating and the reaction time of the atmosphere are two parameters that are especially needed. From an analysis of 3 high inclination satellites, Injun 3, Explorer 19, and Explorer 24, Roemer [10] made some very significant contributions concerning the intensity of heating of the atmosphere for a given level of geomagnetic disturbance. Although considerable scatter exists in his data, his results indicate that the heating level $(\Delta T/\Delta a_p)$ at auroral latitudes is about twice as large as that at the equator. In a study of the reaction time of the atmosphere to heating associated with geomagnetic activity, Roemer compared times at which the rate of change of satellite periods reached their maximum with the times of occurrences of the peak of geomagnetic variations for about 100 geomagnetic events. This analysis indicated a mean time delay time, $\Delta t = 5.3 \pm 0.4$ (s.d.) hours. These average results concerning time delays are in fair agreement with those obtained by Jacchia et al. [8], who analyzed 80 events from 4 high inclination satellites and found an average lag time in the low to medium latitude region ($\phi < 55$ deg) of 7.2 hours, and an average time lag in the high latitude region ($\phi > 55$ deg) of 5.8 hours. There was considerable scatter in these results, with time delays ranging from 0 to more than 14 hours.

Analysis of high-resolution density data deduced from precise radar tracking data from 11 low altitude, attitude-stabilized Agena satellites led to the discovery of delay times of density increases associated with geomagnetic activity from near-instantaneous in the auroral regions ($\phi = 75$ deg) to about 17 hours at lower latitudes ($\phi = 30$ deg) [11]. In this study, 27 events during which the geomagnetic planetary index, a_p, ranged from 12 to 154 units were analyzed. One recognized deficiency in these data was the relatively small eccentricities (0.013 to 0.027) of the orbits of the satellites under consideration. This deficiency increases the angle about perigee through which the drag occurs. It has been noted [8] that the low eccentricities make it difficult to assign a latitude to a drag observation density.

Incorrect conclusions concerning time delays between geomagnetic disturbances and associated atmospheric heating can result from improper smoothing of geomagnetic data. Jacobs [12] analyzed the response time of the atmosphere to geomagnetic disturbances in the 165- to 200-km region of the atmosphere by assuming that the geomagnetic

indices could be represented by 12-hour running means of the 3-hourly geomagnetic index, K_p, appropriate for a time delay for the atmospheric response of 0.23 day. Lew [13] later reanalyzed the same data and found that the actual response time Jacobs had assumed was 0.48 day, because of the manner in which he chose to assign the K_p averages. By averaging the K_p values over a period of 12 hours (4 data points) and assigning the average value to the last time point, Jacobs had inadvertently introduced a time displacement error of about 6 hours. In situ measurements of neutral atmospheric composition and density, which offer time resolutions on the order of seconds as compared to hours for drag-derived data, have recently become available. Taeusch[1] analyzed neutral atmospheric composition variations obtained from a quadrupole mass analyzer during a period in which several geomagnetic disturbances occurred. They found the response of the atmosphere to this activity to be localized in the auroral regions of the earth, with a response time of less than 1 hour. The short response time at the high latitudes is in good agreement with that found by DeVries [11] at comparable latitudes.

LOGACS – AN ORBITAL ACCELEROMETER CALIBRATION EXPERIMENT

One logical means of measuring satellite accelerations caused by atmospheric variations is by an onboard accelerometer. A major difficulty in this measurement method is the difficulty in accurately calibrating the accelerometer for the low accelerations in an orbital environment. To overcome this difficulty, in 1967 the Air Force formulated an experiment to calibrate an extremely sensitive accelerometer in the orbital environment. This experiment is known at LOGACS (LOw-G Accelerometer Calibration System)

The accelerometer selected for the LOGACS flight was the Bell MESA (Miniature ElectroStatic Accelerometer). The MESA is a single-axis, electrostatically pulse-rebalanced accelerometer designed so that both the suspension and rebalance forces can be changed, or scaled, by changing the voltage levels. For this experiment, the Bell MESA was mounted in the aft region of a standard Agena vehicle. The accelerometer was placed on a turntable device so that it could be rotated at two precisely known angular rates or held in two known fixed positions. The Agena vehicle was attitude controlled such that the plane of the turntable was always held in the plane of the local horizon. In its fixed positions, the sensitive axis of the MESA was aligned in the orbital plane (one position in the direction of motion and the other opposite to the direction of motion). Comparison of these measurements

---

1. Taeusch, D. R., Carignan, G. R., and Reber, C. A.: Response of the Neutral Atmosphere to Geomagnetic Disturbances. Paper presented at the XIII Plenary Meeting of COSPAR, Leningrad, USSR, May 20-29, 1970.

allowed accurate determination of the instrument bias. The instrument scale factor was determined by rotating the accelerometer at two distinct rotation rates, approximately 0.5 and 1 rpm. A comparison of measurements obtained in each of these modes permitted accurate determination of the scale factor. Fotou [14] has prepared a detailed description of the instrumentation, data processing methods, results, and other pertinent details concerning the experiment.

The LOGACS experiment was placed into a near-polar orbit on May 22, 1967. During the 18th revolution, 1 day later, the orbit was adjusted such that its apogee altitude was raised to increase the orbital lifetime. The orbital parameters at injection and after the orbit adjustment are given in Table 1.

TABLE 1. ORBITAL PARAMETERS FOR LOGACS AFTER ORBIT ADJUST

Parameter	At Injection	At Revolution 18.4
Date	May 22, 1967	May 23, 1967
Time	1839 GMT	2124 GMT
Height of perigee	148 km	147 km
Height of apogee	357 km	403 km
Inclination	91.5 deg	91.5 deg
Eccentricity	0.015	0.018
Period	89.4 min	89.8 min
Latitude of perigee	43.3 deg N	40.7 deg N

Results of Analyses of LOGACS Data

The successful LOGACS experiment provided approximately 100 hours of acceleration data from which the null bias, accelerometer scale factor, and atmospheric drag on the satellite were calculated. Bruce [15] estimates that the actual errors in the accelerations measured during the LOGACS experiment are less than 1 percent and that the density values deduced from the acceleration measurements are accurate to within ±10 percent. The major source of error is the uncertainty associated with the drag coefficient.

Unexpected geophysical events during the LOGACS experiment were the occurrences of two class 2B solar flares and one class 3B solar flare on May 23, 1967, followed by greatly enhanced geomagnetic activity. Geomagnetic activity was fairly quiet the first portion of the flight, but a large geomagnetic storm, with a geomagnetic index, a_p, value of 256 units, during revolution 44 was followed about 9 hours later by a great geomagnetic storm, with geomagnetic a_p value of 400 for 2 successive 3-hour reporting periods. The values of the 10.7-cm solar radio flux and the geomagnetic planetary index, a_p, during the LOGACS flight are shown in Figure 1, along with the LOGACS orbit numbers during which useful density data were derived.

Comparison of Drag-Deduced and Accelerometer Density Data. The LOGACS vehicle, which also carried an S-band transponder, was tracked accurately by the pulse radar network of the U.S. Air Force Satellite Control Facility. Drag-deduced data during the experiment were computed for comparison with the accelerometer data. The drag-deduced densities and the accelerometer-deduced densities are shown in Figure 2. This graph reveals some interesting differences in the density values obtained by the two methods, such as a difference of about 3.6 hours between the peak density values detected by the accelerometer and those computed from the drag-deduced data during the 2 periods of enhanced geomagnetic activity and differences of density values up to 15 percent between the 2 methods of measurement.

These apparent discrepancies are not surprising, inasmuch as the drag-deduced data are smoothed over periods of several hours and over large distances from the perigee position, while the accelerometer data are near-instantaneous measurements. As would be expected, the accelerometer measurements are much more sensitive to atmosphere variations than are drag-deduced measurements because of their greatly improved time and spatial resolution.

Latitudinal Response of the Atmosphere to Corpuscular Heating. The orbit geometry of the LOGACS experiment provided a unique opportunity to study the atmospheric response associated with geomagnetic activity as a function of geomagnetic latitude. The altitudes of the LOGACS satellite for a typical orbit are shown in Figure 3. During a typical orbit, the satellite was at an altitude of about 300 km at the ascending node, descending to 200 km over the north pole and to about 145 km at perigee, then ascending to about 170 km over the equator and to about 300 km over the south pole.

The highest resolution density data previously available from satellite orbit decay were on the order of about 3 hours, or 2 orbits; LOGACS provided data with a time resolution of 20 seconds – an improvement in time resolution of a factor of more than 500.

During the first 40 orbits of the LOGACS experiment, the geomagnetic activity was low, with the values of the geomagnetic planetary index, a_p, not exceeding 32 units.

Fortunately, they were 7 units or less for 9 hours preceding the 2 large geomagnetic storms that occurred during the flight. The 3-hourly a_p values increased from 4 units at orbit 41 to 56 units 3 hours later and to 236 units 6 hours later. A decrease of a_p values to 154 units followed, with an increase to 400 units during orbit 51.

For this analysis of density increases associated with the enhanced geomagnetic activity during the LOGACS experiment, density data subsequent to orbit 41 were normalized to the geomagnetically quiet conditions occurring during orbit 41. The ratios of the normalized densities as a function of geomagnetic latitude were then plotted for all orbits for which data were available.

The satellite positions corresponding to the left sides of Figures 4 through 9 were near the ascending node of the orbit, or the points at which the satellite crossed the equatorial plane in a northerly direction. At these positions, the satellite would be at an altitude of about 300 km. The first crossing of the northern hemisphere auroral zone would occur on the night sector, near 65 to 70 deg geomagnetic latitude, at an altitude of about 190 km. After crossing the north pole, the satellite would cross the auroral zone on the sunlit side of the hemisphere. The satellite was in a near sun-synchronous orbit, with a local time at perigee of about 10:30. Ratios of the density at each revolution to that occurring during revolution 41 are shown in the upper part of the ordinates of Figures 4 through 9. The altitudes of the satellite are shown in the bottom part of the ordinates, with the geomagnetic latitudes shown in the abscissas of Figures 4 through 9.

Figure 4 shows the graph of the normalized density versus geomagnetic latitude during revolution 43, at which time the value of the a_p index had increased to 56 units. In general, the density values had not changed more than a few percent at geomagnetic latitudes less than 50 deg. However, the density at a geomagnetic latitude of about 75 deg (on the dark side of the northern hemisphere) had increased about 30 percent; while that at the sunlit side of the northern hemisphere at the same latitude, they had decreased about 20 percent. This is a rather surprising result, since the most widely accepted atmospheric models such as the Jacchia [16] and CIRA [17] would indicate global heating about 6 hours subsequent to the enhanced geomagnetic activity.

Figure 5 shows the neutral density enhancement during revolution 46, approximately 1.5 hours subsequent to the peak of the first large geomagnetic storm, during which the a_p value reached 256 units. Again, the highest relative increase of density during this orbit occurred at about 70 deg geomagnetic latitude on the night side of the northern hemisphere. A very small (about 5 percent) increase of density occurred at 70 deg geomagnetic latitude on the sunlit side; however, significant increases occurred at higher geomagnetic latitudes in the southern hemisphere. This indicates that the immediate source of heating is near the auroral zone on the night side of the northern hemisphere and near the auroral zone in the southern hemisphere.

Figure 6 shows the normalized density values during revolution 47, about 3 hours subsequent to the peak of the first geomagnetic storm. in general, density values at lower latitudes were starting to increase (by about 20 percent), while those in the auroral regions were decreasing.

Figure 7 shows the normalized density ratios at about 4.5 hours subsequent to the first geomagnetic storm. By this time, density values near the equator had increased about 50 percent, while those near the auroral regions on the night side of the northern hemisphere had decreased to values near those at geomagnetically quiet times. One very interesting feature illustrated in Figure 7 is the decrease of density over the polar cap and in the auroral regions to values 20 to 30 percent below those occurring before the enhanced geomagnetic activity.

Approximately 9 hours after the peak geomagnetic index values for the first geomagnetic storm had been reached, one of the largest disturbances of solar cycle 19 occurred, with values of the geomagnetic index, a_p, reaching 400 units for two consecutive periods. Figure 8 shows ratios of densities at the beginning of this high geomagnetic activity to those occurring during the geomagnetically quiet period 18 hours previously. Again, the significant density increases were localized near the geomagnetic latitude of 65 deg on the dark side of the northern hemisphere and near 60 deg in the observations available from the southern hemisphere. In both cases, values of density increased by more than a factor of two, almost simultaneously with the increase of geomagnetic activity. An examination of the satellite altitudes at which the highest density ratios were evident reveals no noticeable altitude dependence, since the satellite was at an altitude of about 190 km during the northern hemisphere traverse of the night auroral zone and at an altitude of about 265 km during the period of enhanced density values in the southern hemisphere auroral zone. Again, there was a decrease of density to below geomagnetically quiet values at a geomagnetic latitude of about 65 deg on the sunlit side of the northern hemisphere. Density values near low altitudes, at this time, had not changed significantly from slightly enhanced values associated with the previous geomagnetic activity.

The latitudinal variations of density changed considerably within the next 4.5 hours, as shown in Figure 9. Although the a_p index during this orbit had remained at 400 units, the atmospheric density decreased to near-normal values in the auroral region, but had increased by more than a factor of about two in equatorial regions. Peak density ratios had thus moved from 65 deg latitude to 20 to 30 deg latitude during the 4.5-hour period, although there had been no decrease in geomagnetic activity. At the auroral latitudes on the sunlit side of the northern hemisphere, the density had decreased to about 75 percent of that occurring before the onset of geomagnetic activity.

Dependence on Time Delays for Atmospheric Heating on Geomagnetic Latitude and Altitude. During the 36-hour period for which density values were available from the LOGACS experiment, following the onset of enhanced geomagnetic activity, density values were obtainable from all or portions of 20 orbits. These data presented a unique opportunity

to evaluate effects of geomagnetic latitude and altitude on the time required for the neutral atmosphere to respond to the heating associated with geomagnetic activity. Density data normalized to the geomagnetically quiet period preceding the high geomagnetic activity, as described in the previous section, were tabulated at intervals of 10 deg geomagnetic latitude for each available orbit. Time cross sections for each 10 deg of geomagnetic latitude were then prepared for the entire period. Since an orbital period was about 90 minutes, this was the minimum time resolution attainable. The longest time resolution during the period under consideration was three orbits, or about 270 minutes. Time cross sections of normalized density values at intervals of 10 deg geomagnetic latitude are shown in Figures 10 and 11. Corresponding values of the geomagnetic index, a_p, are shown at the bottom of the figures. Time delays between the peak of the a_p values for each of the 2 large geomagnetic events that occurred during this period (assumed at the middle of the 3-hourly a_p reporting periods) and the peak values of the normalized density associated with each event are shown for all cases in which adequate data were available to make this evaluation.

An analysis of these time delays strongly supports the earlier conclusions by DeVries et al. [11] that time delays between the onset of geomagnetic activity and the subsequent enhancement of atmospheric heating are latitude dependent. For example, at geomagnetic latitudes greater than 60 deg, these time delays were, in every case, not more than 1.5 hours; at geomagnetic latitudes less than 30 deg, they were, in every case, not less than 4.5 hours. Between these latitudes, the time delays were about in proportion to the decrease in geomagnetic latitudes.

The time differences between the peak of the geomagnetic disturbances and the associated atmospheric heating for the 30 cases for which data were available are shown in Figure 12. Corresponding altitudes are shown in parentheses. It can be seen from Figures 12, 5, and 8 that the time delays are about independent of altitude but are strongly dependent upon geomagnetic latitude.

The serial correlation coefficient of geomagnetic latitudes with lag times for the 30 cases is 0.834, which is less than the 0.001 level of statistical significance. In other words, the probability of exceeding this value by chance is less than 1 in 1000. The line of least squares fit, as shown in Figure 12, is based upon the relationship:

$$T = \frac{70.4 - \text{Geomagnetic Latitude}}{9.4} \qquad (2)$$

where T is the lag time in hours.

The Similarity Between the Locations of the Auroral Electrojet and Spatial Density Variations Detected During the LOGACS Experiment. Auroral electrojets are intense electric currents in the auroral zones associated with geomagnetic disturbances. Blumen et al. [18] summarize the general features of the auroral electrojet to consist of a height of the jet axis varying from 100 to 150 km, a length from 2000 to 5000 km, north-south thickness from 500 to 680 km, vertical half-width of 30 km, and a duration of 30 to 60 minutes. Akasofu et al. [19] discuss the morphology, geometry, and current system of the auroral electrojet. If the mechanism for atmospheric heating associated with geomagnetic disturbances is Joule heating, according to Cole [6], the magnitude of such heating will be a function of the electrical current in the ionosphere with major concentration in the auroral latitudes. Accepting this hypothesis and a model current system for an intense polar magnetic substorm similar to one depicted by Akasofu et al. [19], the most intense heating should occur in the auroral zone of the midnight sector of the hemisphere.

A proposed model current system for an intense magnetic substorm and the corresponding traverse of the LOGACS experiment through the system are shown in Figure 13 [19]. LOGACS experiment revolutions 46 and 51 occurred shortly after the onsets of 2 intense geomagnetic disturbances. Figures 5 and 8 show the immediate atmospheric density enhancements associated with this activity. The portion of the orbit in Figures 5 and 8 which corresponds to the track shown in Figure 13 includes the region from geomagnetic latitudes of +50 deg to +90 deg, then back to +50 deg. Figures 5 and 8 with the orbital track shown in Figure 13 show an interesting pattern of density enhancements which resembles, to a remarkable extent, that which would be expected with the current system in Akasofu's model. In both cases, the most intense enhancement of density occurs coincident with the most intense portion of the electrojet current system penetrated by the satellite (Point A, at about 70 deg geomagnetic latitude at an altitude of 190 km in Figure 5 and at about 75 deg geomagnetic latitude and an altitude of about 190 km in Figure 8). The portions of the orbits shown in Figures 5 and 8 from point B to point C (75 to 50 deg geomagnetic latitude on the sunlit side of the hemisphere) show no significant enhancement of density even though they are in proximity to the auroral oval. An examination of this region in Akasofu's model (Fig. 13) shows there is no enhancement of the current system in this region; therefore, Joule heating would not provide the mechanism for heating on this portion of the orbits.

Unexpected anomalies, which are shown between points D and E in Figure 7 (about 4.5 hours subsequent to the commencement of the first geomagnetic storm) and Figure 9 (about 4.5 hours subsequent to the commencement of the second geomagnetic storm), occur in regions in which the density decreased to values as low as 70 percent of pre-storm values. The geographic regions in which this phenomenon occurs appear to be within the auroral oval. The apparent density depletion may result from the circulation and wind patterns associated with the high geomagnetic activity occurring a few hours previously.

Evidence of Wave Propagation from LOGACS Data. In a study to evaluate the capability of various atmospheric models to depict atmospheric density for geomagnetic conditions during the LOGACS flight, cross sections of the ratios of the actual density to the density depicted by various models as a function of geomagnetic latitude were prepared. Figure 14 shows such a cross section during the period subsequent to the second geomagnetic storm. These data indicate evidence of atmospheric waves. General features of these waves include wavelengths on the order of 450 km and amplitudes of the ratio of the actual density to that depicted by the model increasing with altitude. It seems plausible that the source of this apparent wave motion is Joule heating associated with the geomagnetic storm. Such a wave would most likely propagate radially from the auroral electrojet. The satellite descended in altitude as it moved north through the wave region and the wavelength is a combination of vertical and horizontal variations. It is noteworthy that the amplitude of the wave decreased as the altitude decreased. As the wave propagates from the source it will tend to conserve kinetic energy and the amplitude will decrease on the portion of the wave front that is propagating into the more dense layers and increase on the portion of the wave that is propagating upward into the less dense layers. Theoretical studies on the phenomena are being conducted in collaboration with Dr. George H. Fichtl of the NASA/MSFC Aerospace Environment Division.

Inadequacy of Currently Available Atmosphere Models to Depict Density Variations Associated with Large Geomagnetic Disturbances. The most widely accepted model of the atmosphere, the Jacchia Model [16], approximates temperature increases (with a lag of 6 hours) associated with geomagnetic activity by equation (1). Actual density increases are then computed from a model. The maximum temperature correction by this method for the largest geomagnetic storm that can be measured is about 500 deg. While this temperature correction appears to be adequate to increase the densities sufficiently at altitudes above about 250 km, it is impossible to accurately model density increases associated with large geomagnetic disturbances at altitudes below about 200 km by this technique. Figure 15 shows the extremes of density measured by the LOGACS experiment between altitudes of 145 and 290 km, compared to those depicted by the most recent Jacchia Model [16], assuming exospheric temperatures of 1000, 1500, and 2000 deg. Figure 15 shows that maximum density values observed during the LOGACS experiment when the a_p value was 400 units are higher than those depicted by the Jacchia 2000-deg exospheric temperature model at all altitudes up to 290 km, with the percentage differences being larger at lower altitudes. In other words, all observed density values when a_p was 400 units lie outside the limits of those depicted by the Jacchia Model.

The method used by Jacchia and others to study the magnitude of atmospheric variations is to convert the density variations, as depicted by satellite drag, to temperature variations to relate events at different altitudes to each other. This transformation is only as accurate as the atmospheric model being used for the transformation. One of the major shortcomings of the currently available atmospheric models, including Jacchia's [16], is that they assume static equilibrium conditions which we know do not exist during the short-period atmospheric perturbations occurring during a geomagnetic storm.

The second major problem in the modeling of atmospheric variations associated with geomagnetic activity is that of depicting the reaction time of the atmosphere. Current models are designed on the premise that the atmosphere reacts on a global basis with a time lag of 6 hours subsequent to the geomagnetic activity. Analyses of LOGACS data indicate that neither assumption is entirely correct; i.e., the atmosphere responds nearly simultaneously with the onset of geomagnetic activity near the auroral zones, with this energy being propagated to lower latitudes by wave mechanisms, and/or conduction and convection with a time delay of about 6 hours near the equator.

Based upon these data, the modeling of atmospheric variations associated with geomagnetic disturbances can be improved by incorporating a variable time delay (near-simultaneous at the auroral region and increasing to 6 hours at the equator) and by directly modeling the density perturbations as a function of geomagnetic activity near the altitude region where the heating occurs (below 140 km). Research on this problem is in process at the MSFC Aerospace Environment Division. Additional data from other accelerometer flights will be quite valuable for this effort.

CONCLUSIONS

The LOGACS experiment probably furnished more evidence from which to evaluate the mechanism responsible for atmospheric heating associated with geomagnetic activity than any other data. Analyses of these data indicate Joule heating as the principal mechanism for such atmospheric response. This conclusion is supported by the following observational evidence from the LOGACS experiment:

1. There is a response of the atmosphere in the auroral regions nearly coincident with the onset of geomagnetic activity, with no significant response evident at lower latitudes until several hours later.

2. There is a high correlation between the times of peak geomagnetic activity and the geomagnetic latitudes at which the maximum heating of the neutral atmosphere occurred. This relationship indicates that heating associated with the geomagnetic activity originated in the auroral region and propagated systematically to lower latitudes.

3. The maximum atmospheric heating occurred at geographic locations near the expected maximum current of the auroral electrojet. This would be expected with Joule heating, since Q, or energy from such heating, is directly proportional to the square of the auroral electrojet current.

4. Strong evidence of atmospheric wave propagation was present only during short periods subsequent to enhanced geomagnetic activity. These waves appear to originate in the auroral region at altitudes commensurate with a source associated with Joule heating.

5. A decrease in atmospheric density in the auroral regions occurred 4 to 5 hours after commencement of the high geomagnetic activity, during a period in which the geomagnetic activity remained highly enhanced. This indicates atmospheric circulation associated with extremely high pressure gradients and winds which would be expected with Joule heating.

Presently available atmospheric models do not depict adequately the atmospheric response to geomagnetic activity, particulary at low (below 200 km) altitudes. This is not surprising, since these models are based upon the assumption of equilibrium conditions, which are known not to exist during transient atmospheric disturbances. Atmospheric models can be improved by incorporating an atmospheric response near the altitude at which the heating occurs, with a latitude-dependent magnitude and a time delay.

George C. Marshall Space Flight Center
National Aeronautics and Space Administration
Marshall Space Flight Center, Alabama 35812, February 10, 1971
976-30-00

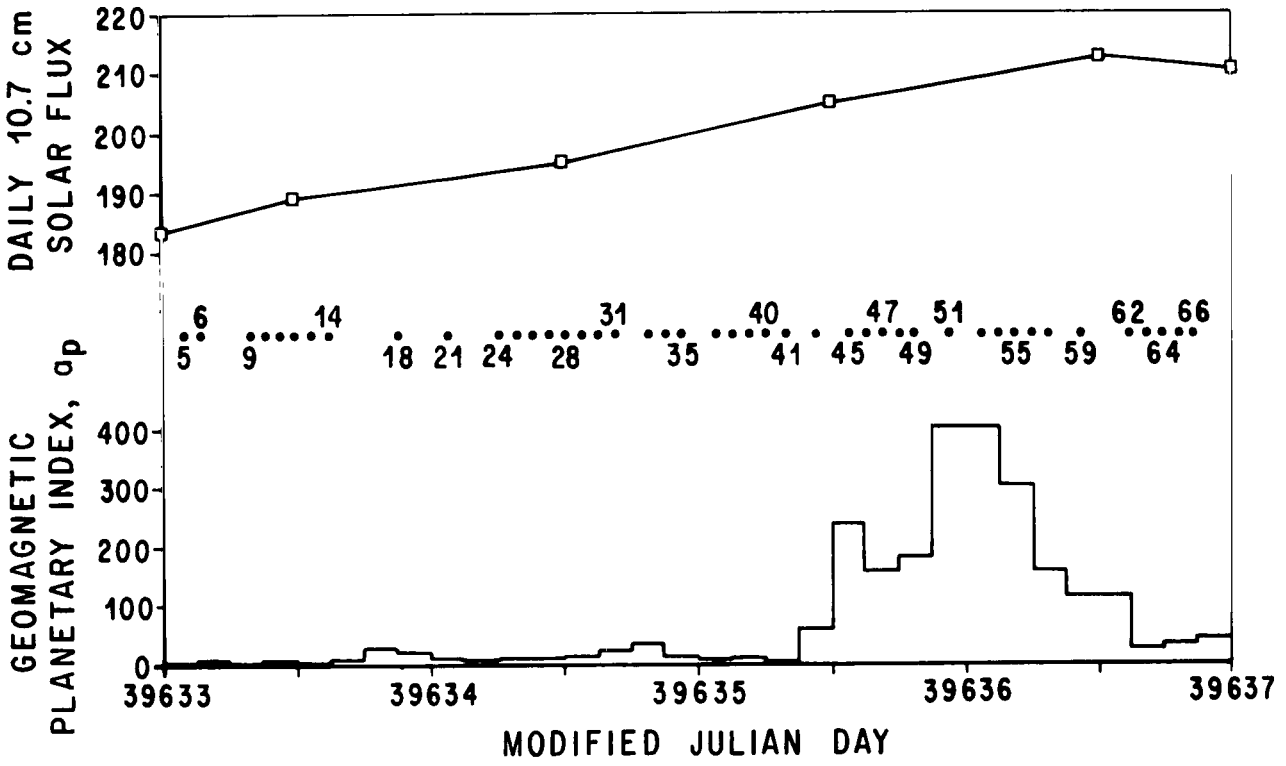

Figure 1. Variations in the daily 10.7-cm solar radio flux and the geomagnetic planetary index, a_p, during the LOGACS experiment, with corresponding revolutions during which useful density data were obtained.

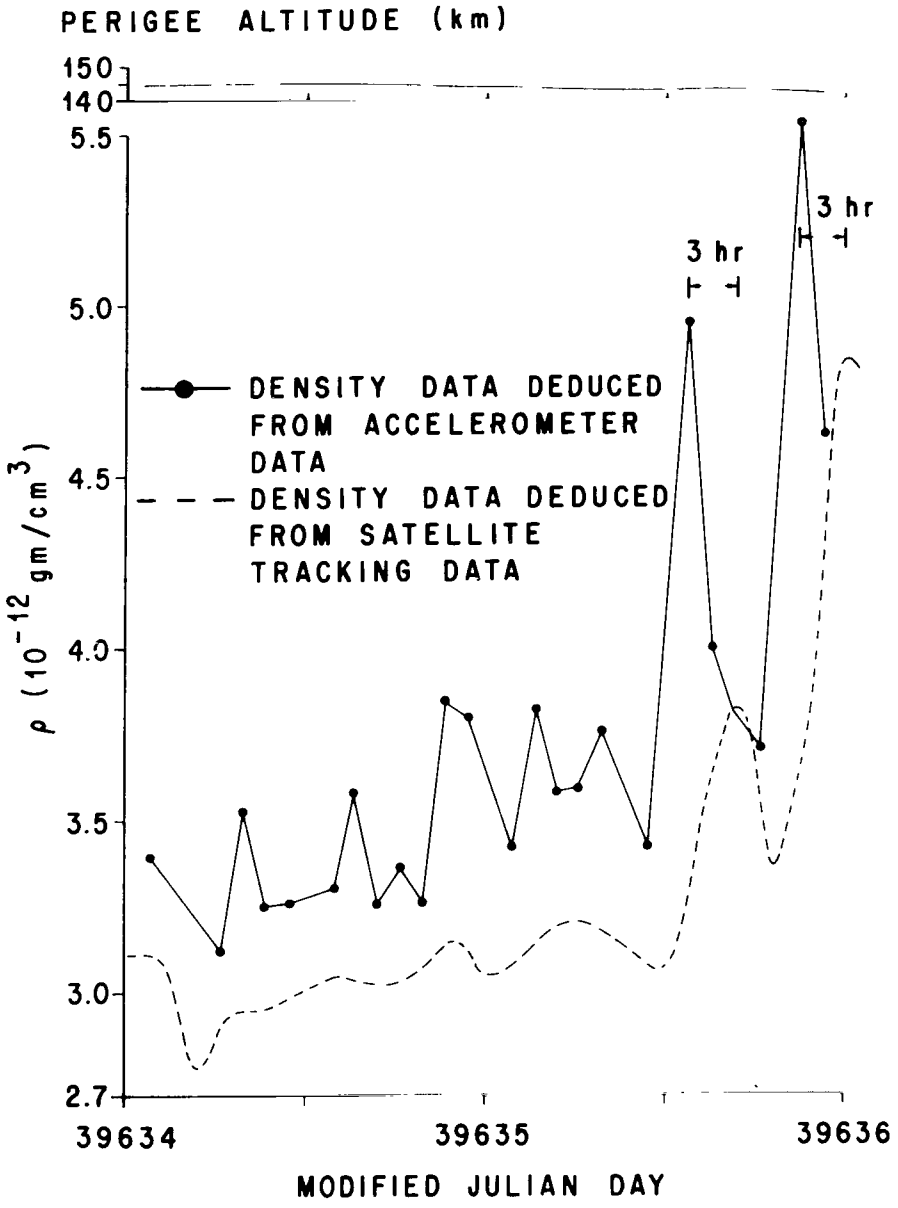

Figure 2. Comparison of density deduced from tracking data during the LOGACS flight with density deduced from accelerometer data.

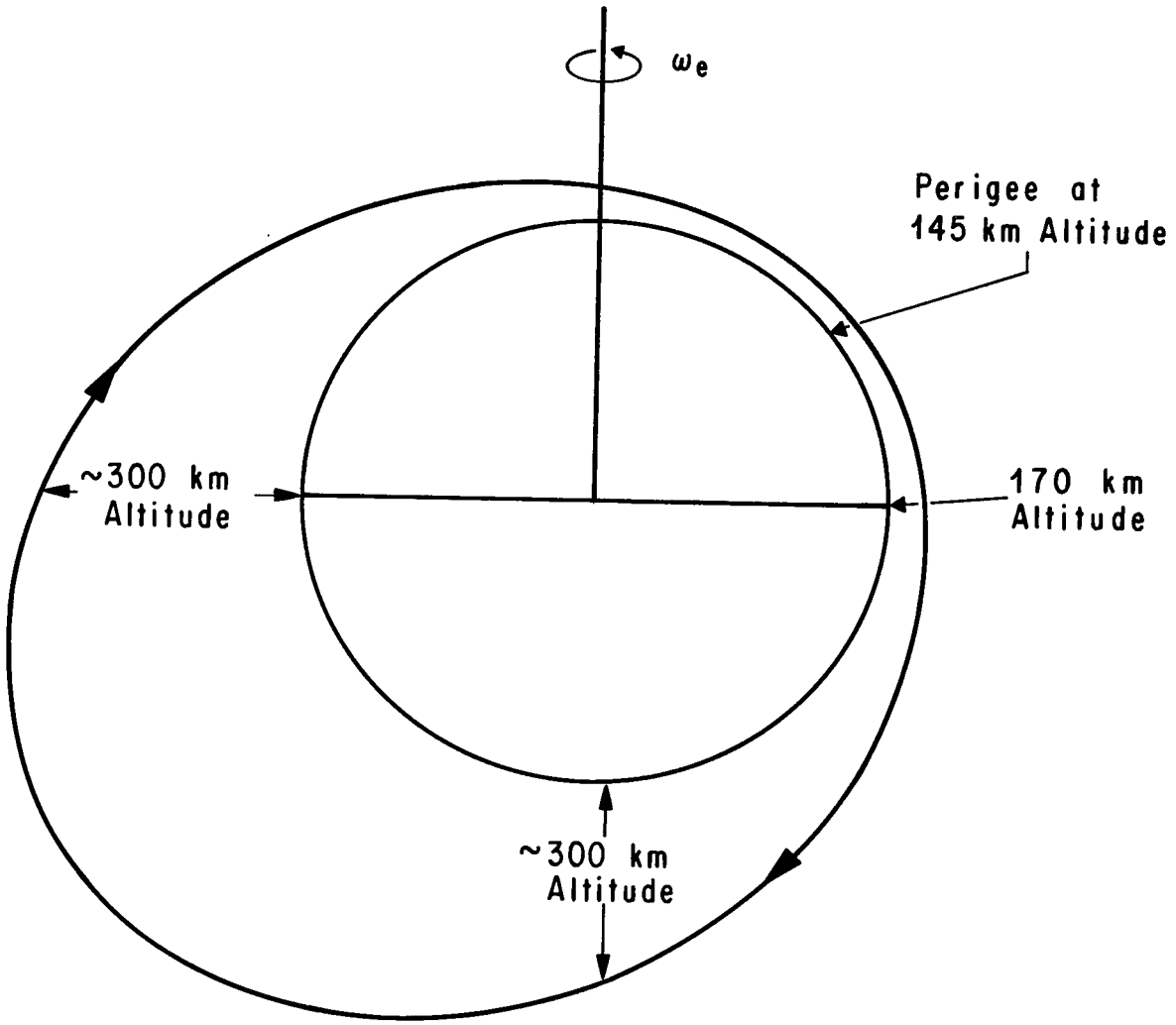

Figure 3. LOGACS orbit geometry.

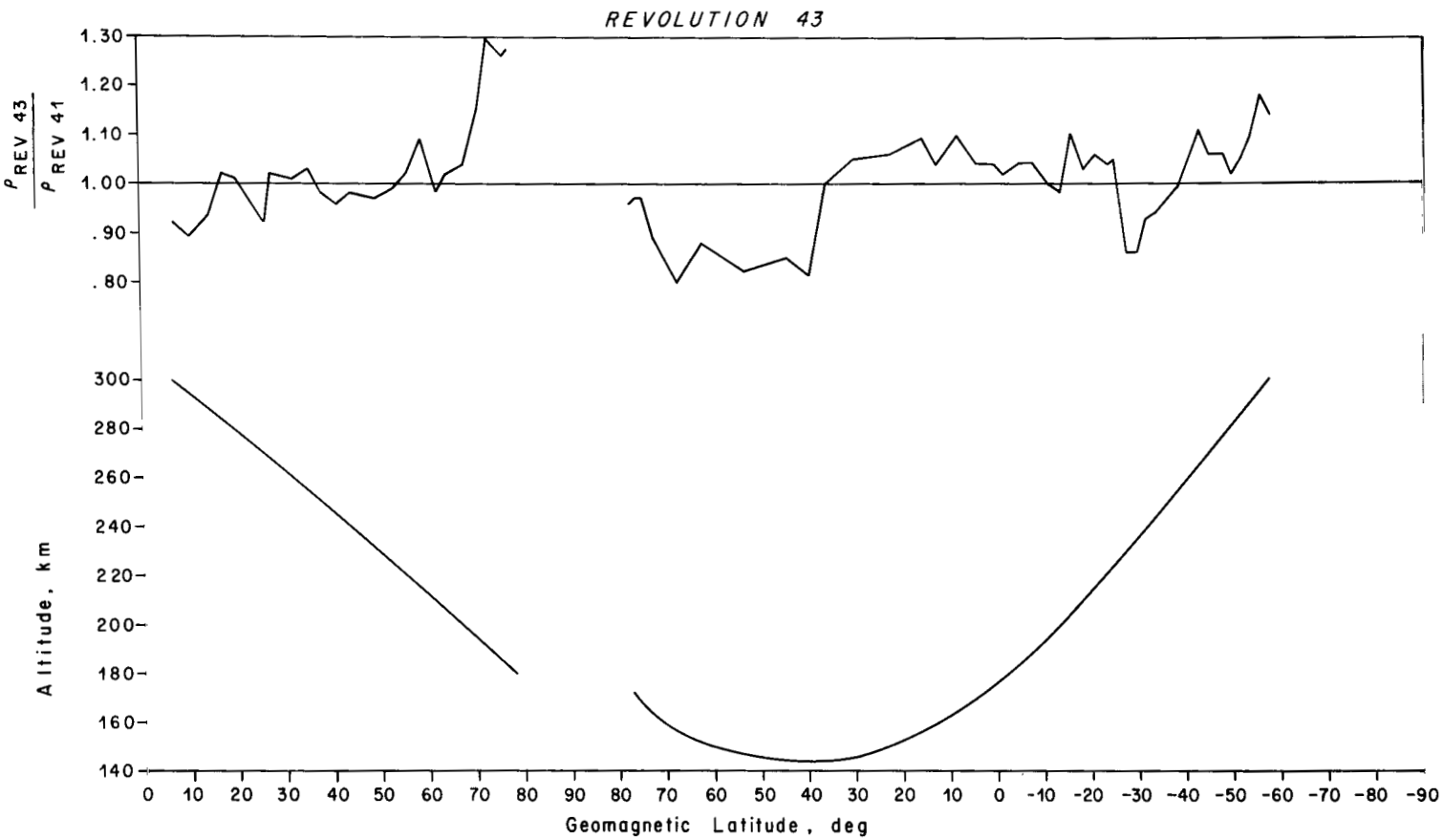

Figure 4. Normalized density values versus geomagnetic latitudes during revolution 43, $a_p = 56$.

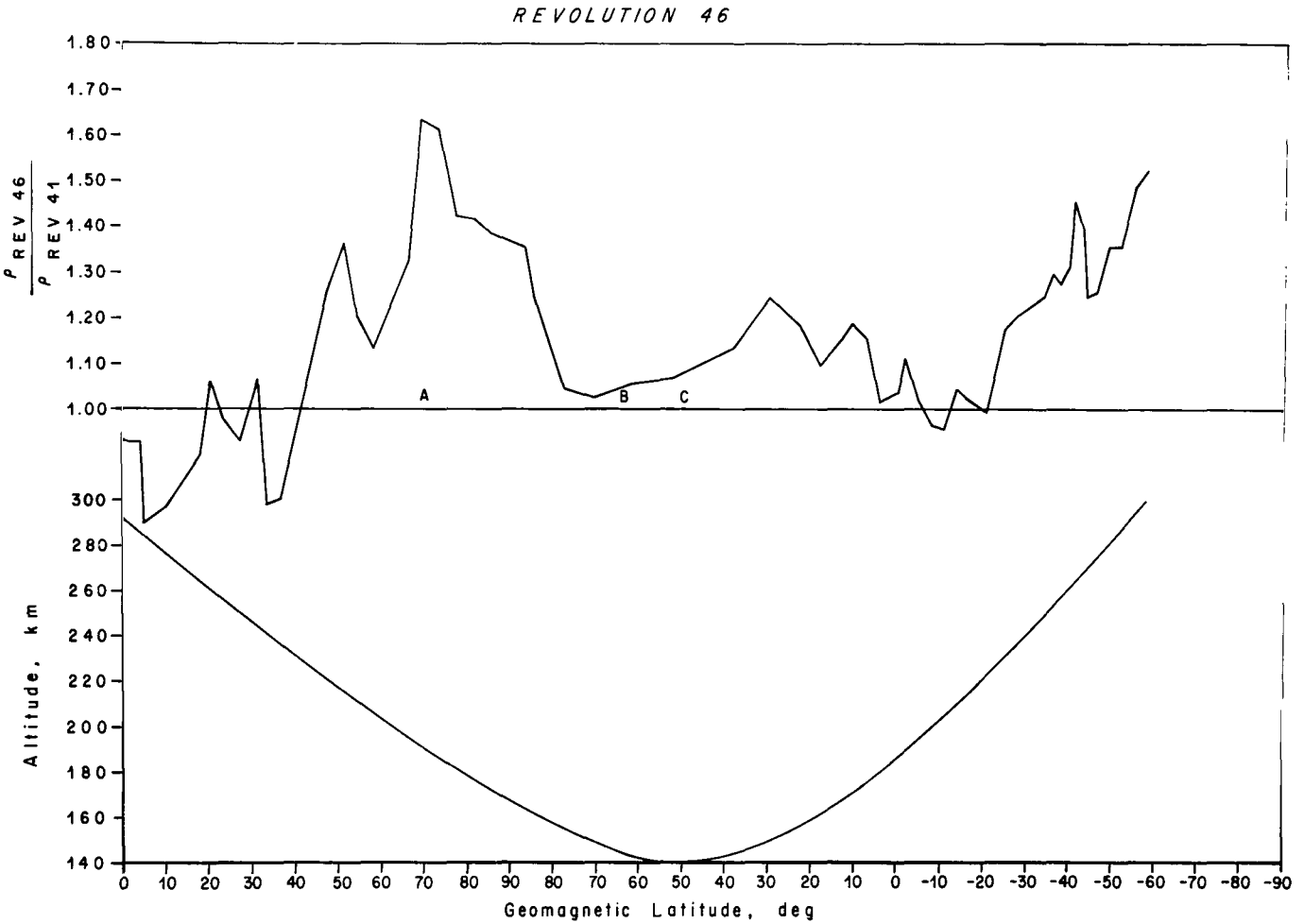

Figure 5. Normalized density values versus geomagnetic latitudes during revolution 46, 1.5 hours after $a_p = 256$.

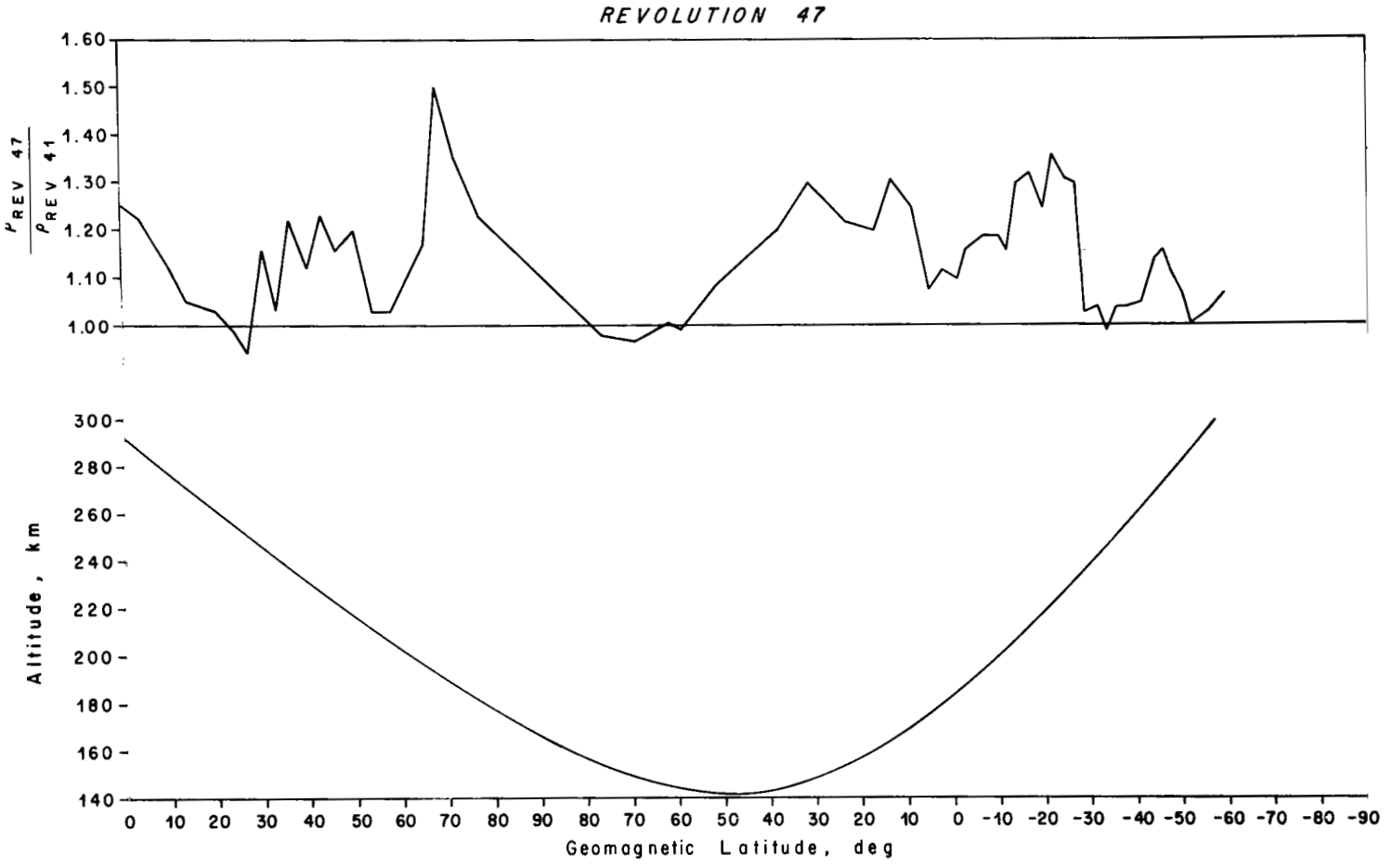

Figure 6. Normalized density values versus geomagnetic latitudes during revolution 47, 3 hours after $a_p = 256$.

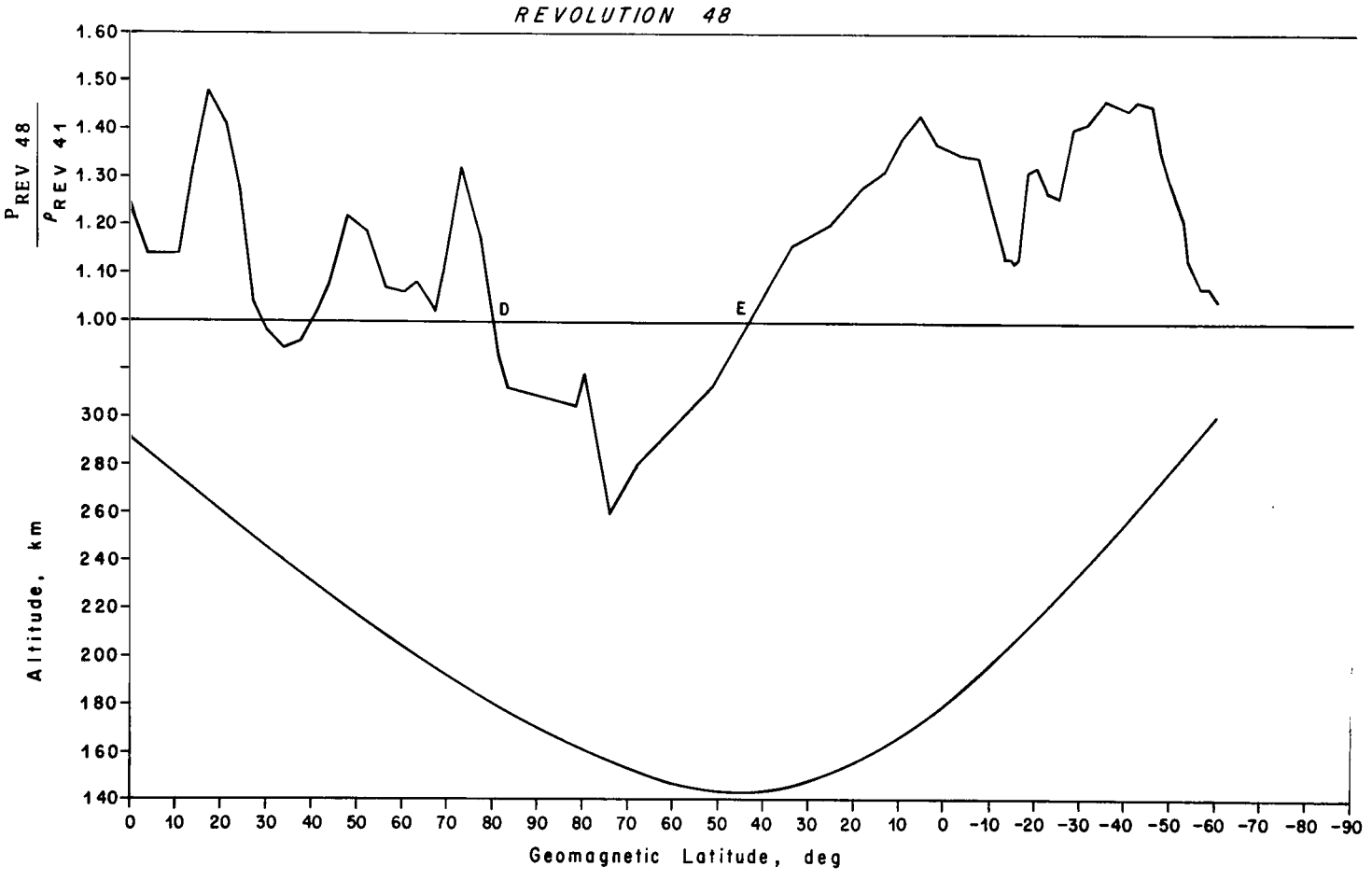

Figure 7. Normalized density values versus geomagnetic latitudes during revolution 48, 4.5 hours after $a_p = 256$.

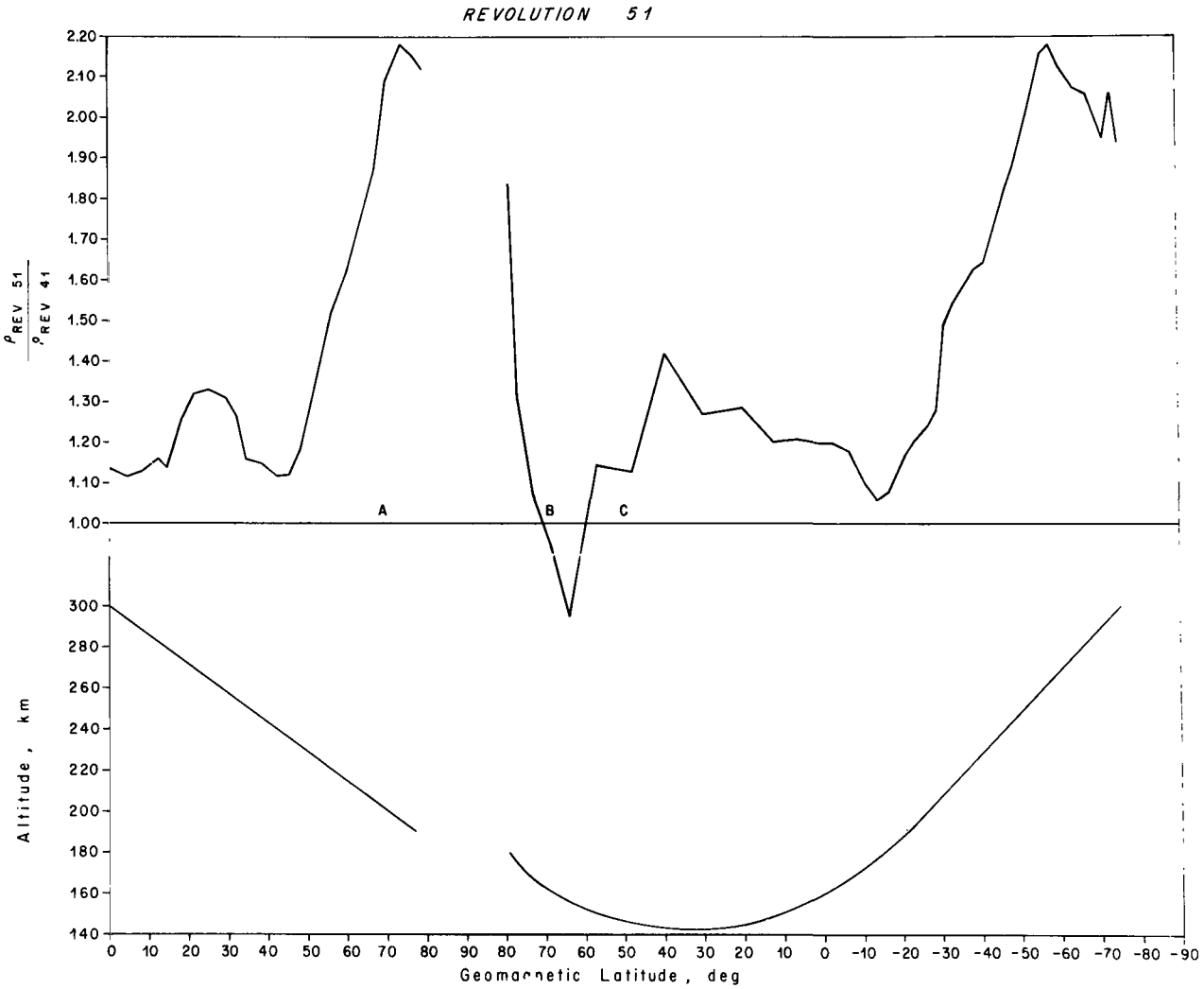

Figure 8. Normalized density values versus geomagnetic latitudes during revolution 51, $a_p = 400$.

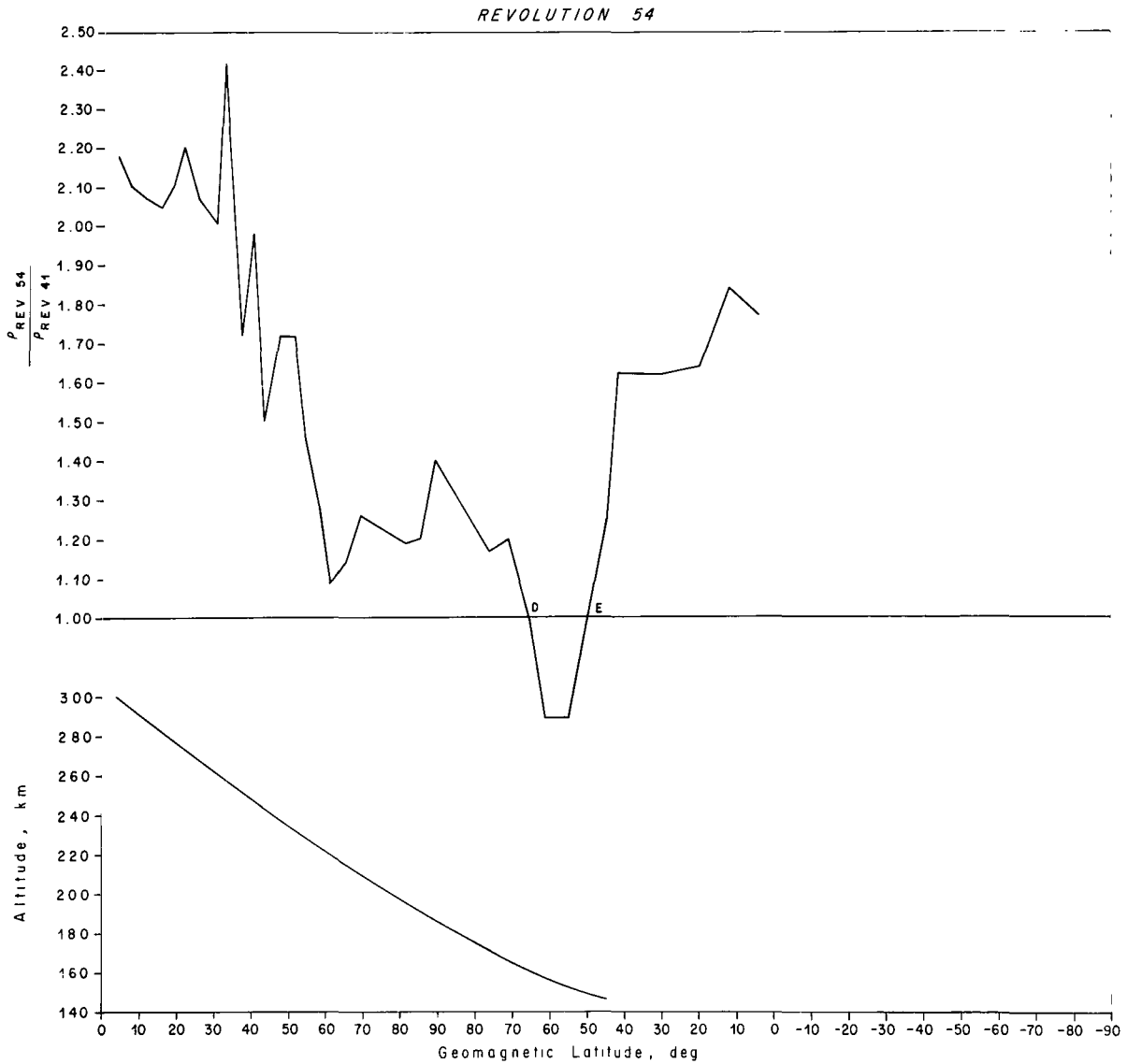

Figure 9. Normalized density values versus geomagnetic latitudes, 4.5 hours after a_p reached 400.

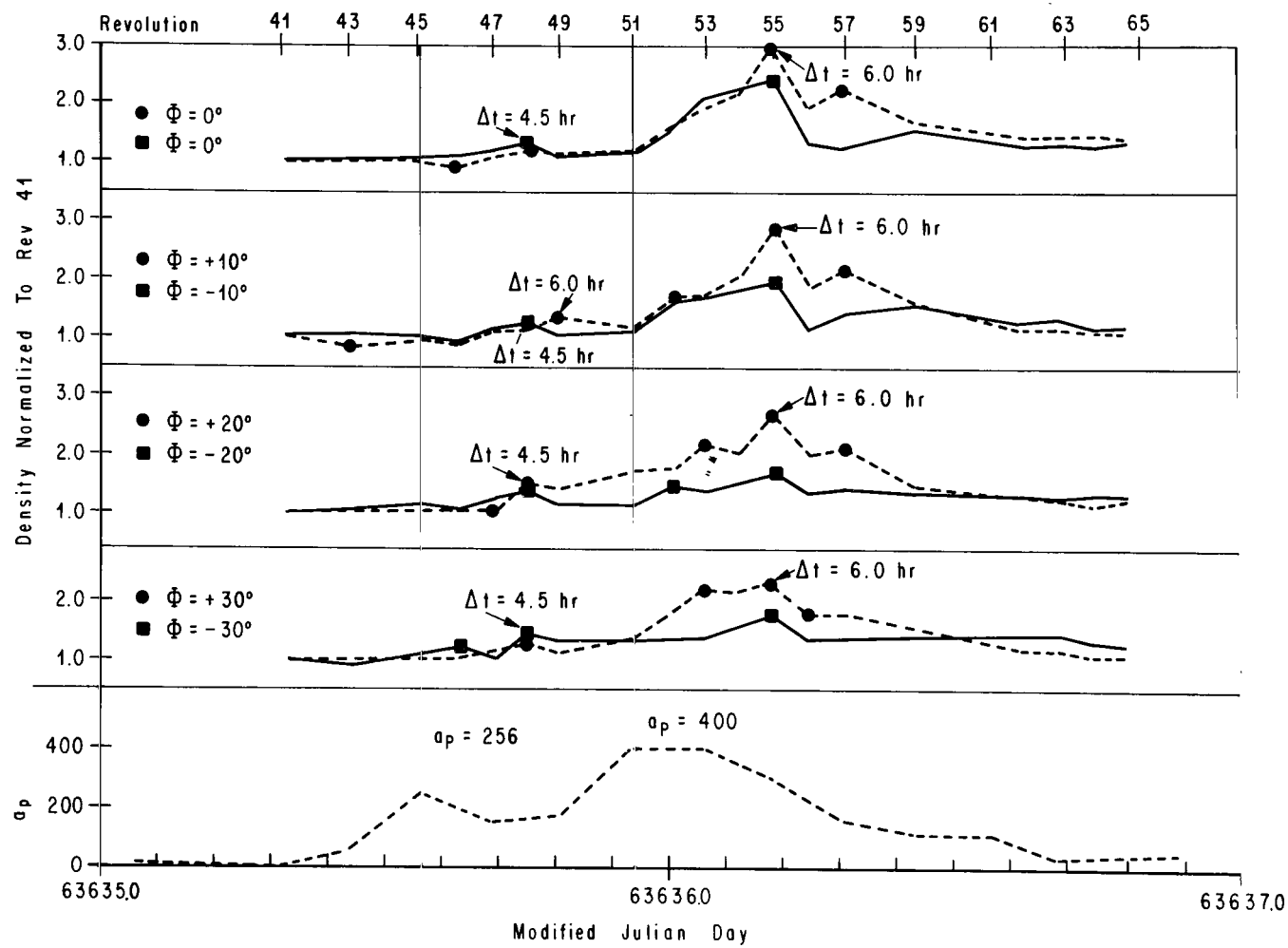

Figure 10. Time cross sections of normalized density values at 10 deg of latitude intervals, Φ = 0 to ±30 deg geomagnetic latitude.

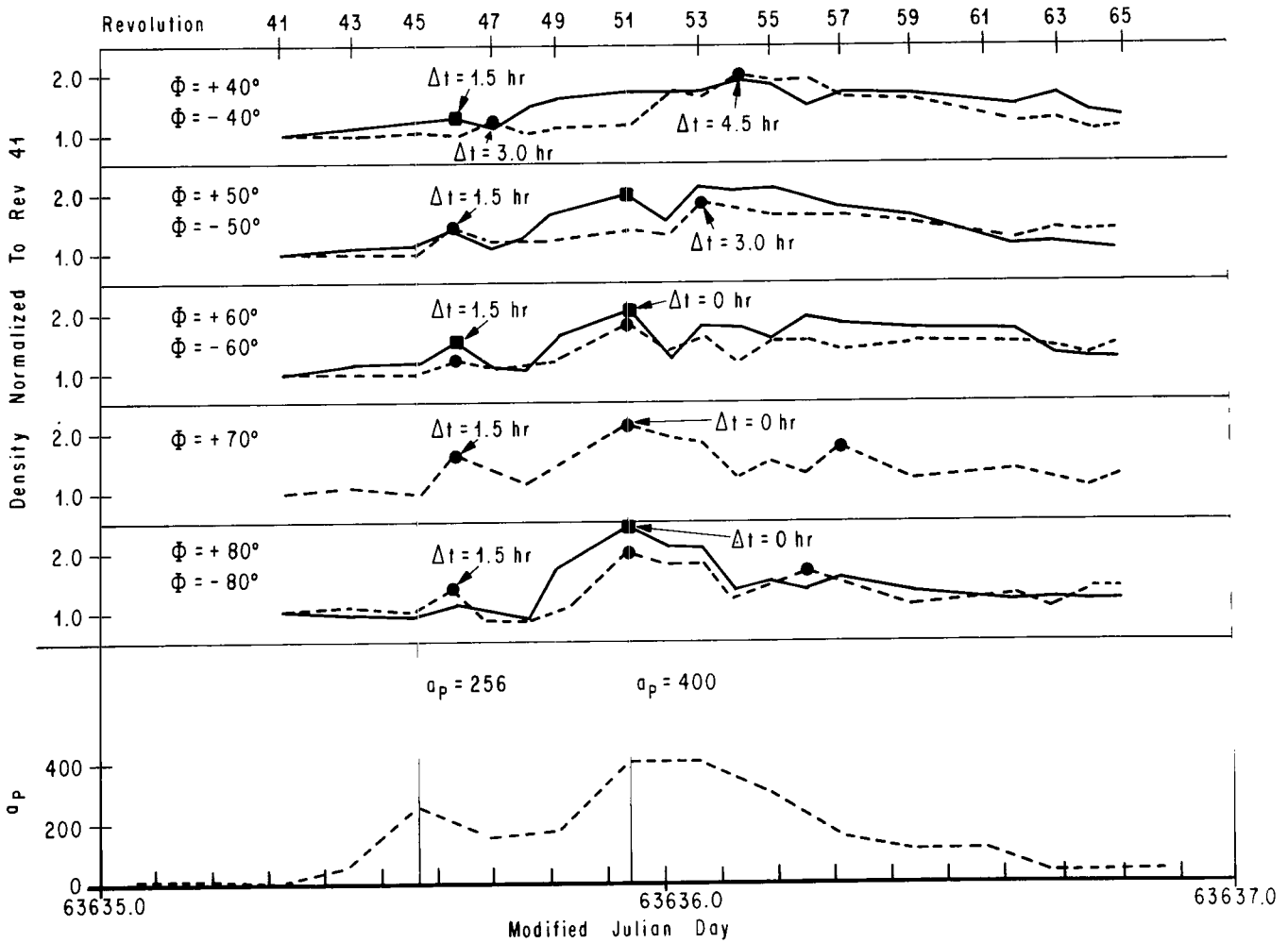

Figure 11. Time cross sections of normalized density values at 10 deg of latitude intervals, $\Phi = \pm 40$ to ± 80 deg geomagnetic latitude.

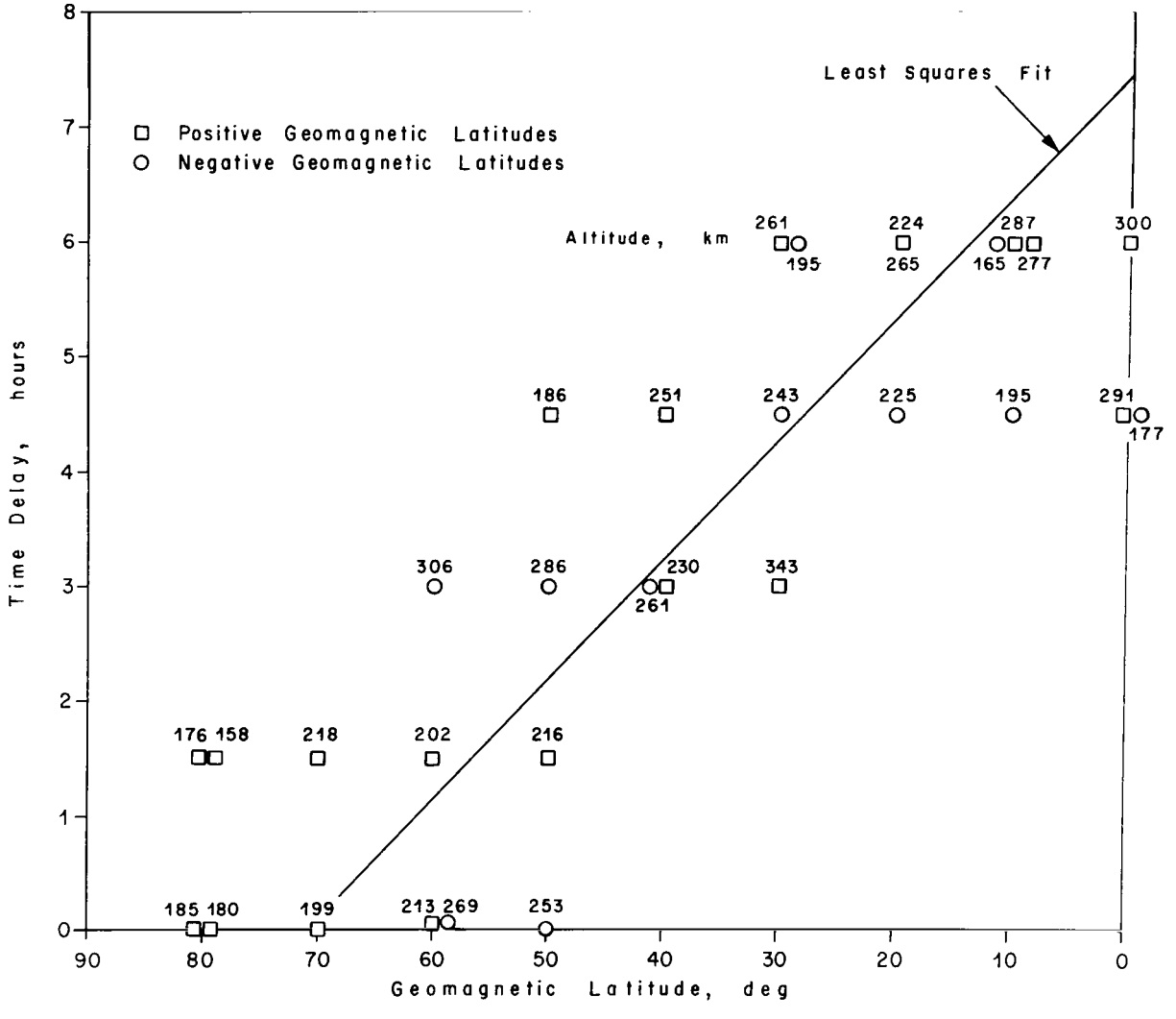

Figure 12. Time delays between the peaks of geomagnetic disturbances and associated atmospheric increases.

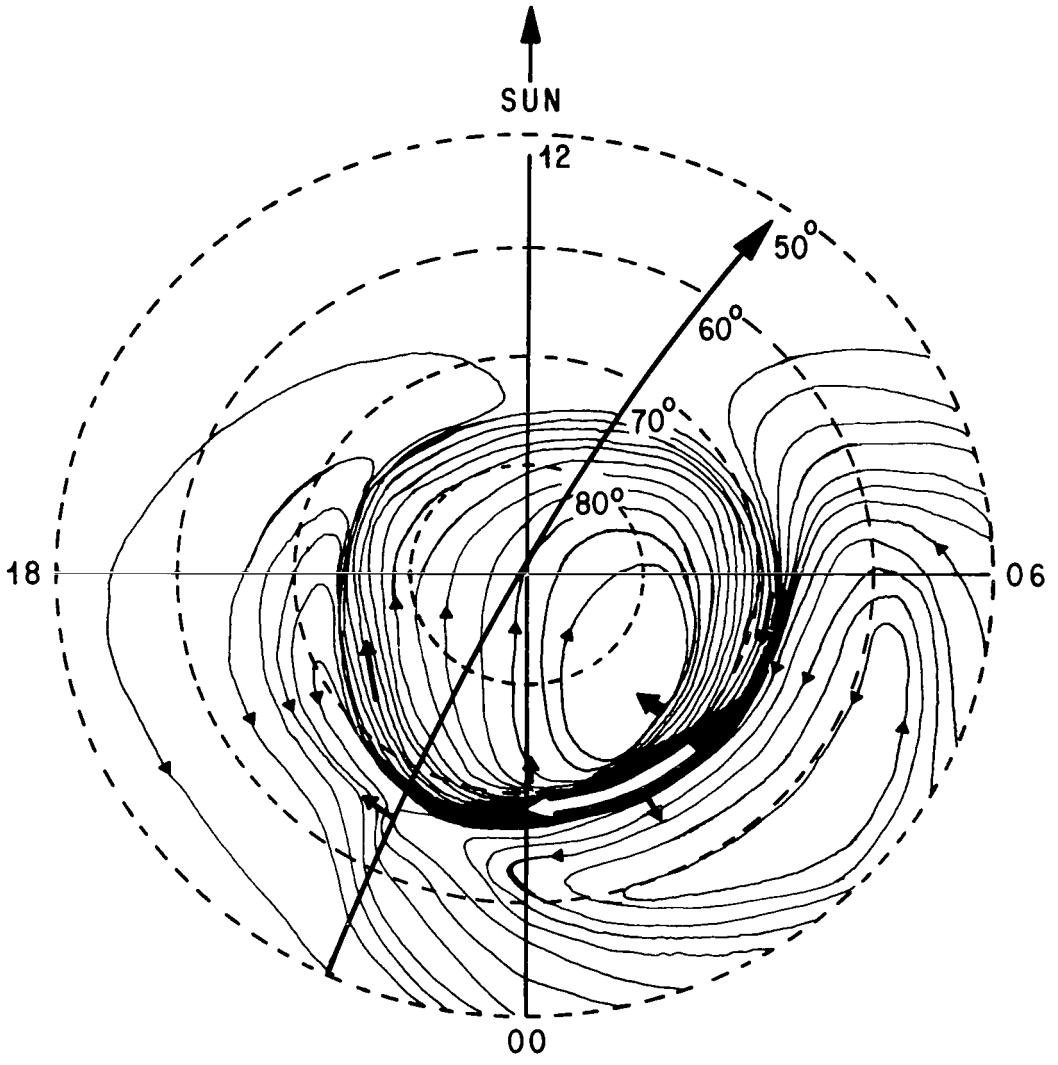

Figure 13. Proposed model current system for intense polar magnetic storms, with the corresponding LOGACS track. (After Akasofu [19]).

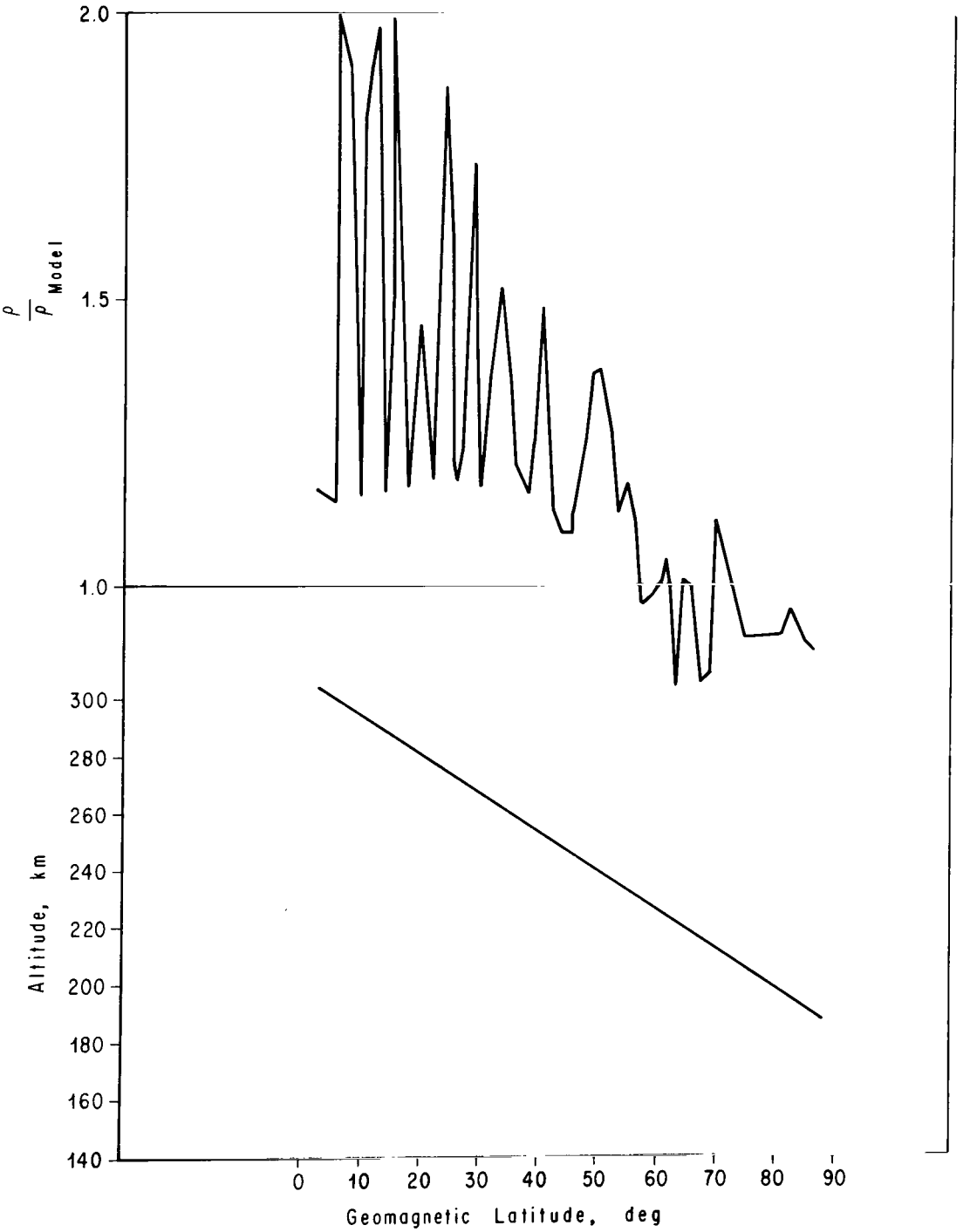

Figure 14. Evidence from LOGACS data of atmospheric wave propagation.

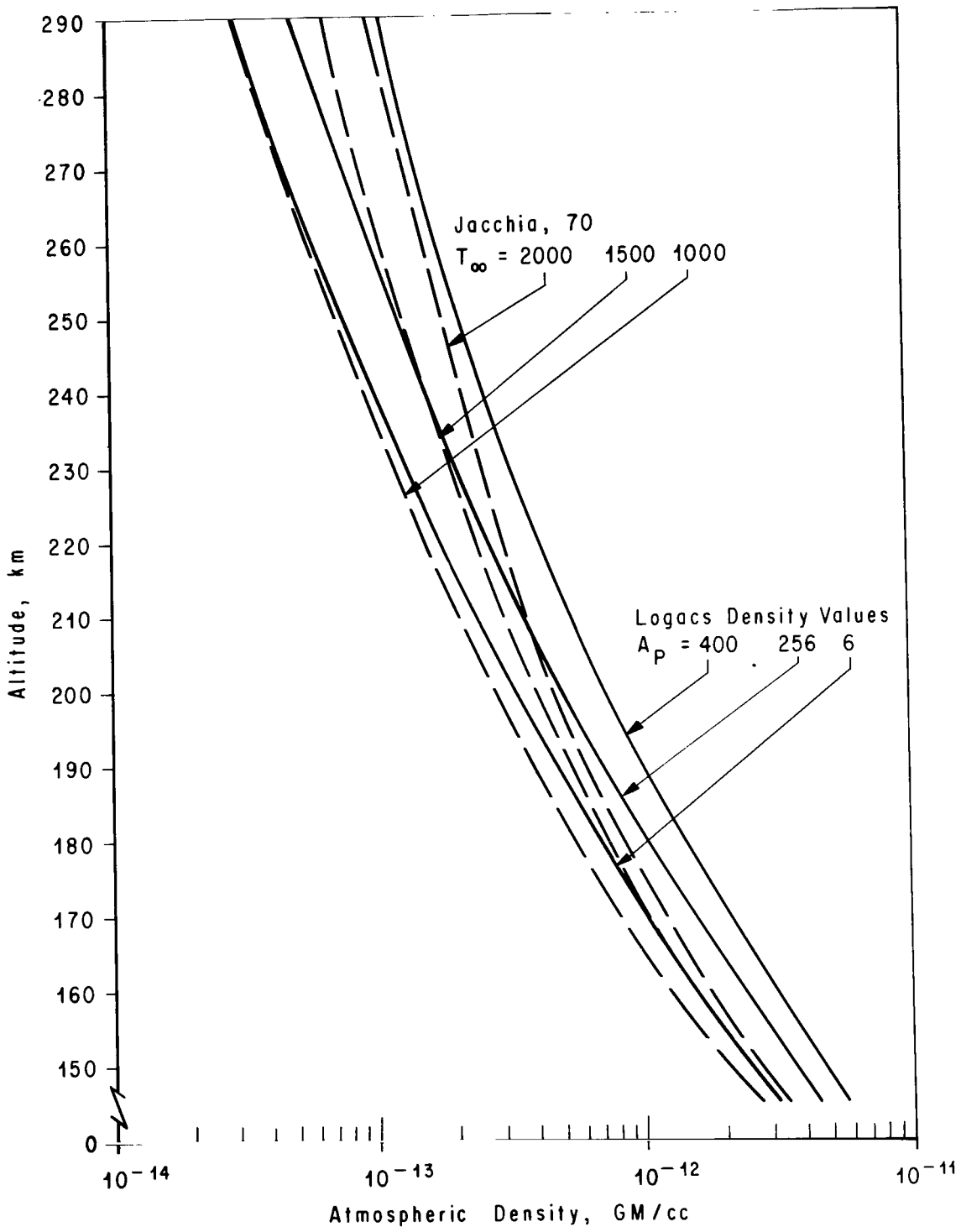

Figure 15. Extreme values of density depicted by the Jacchia 70 atmosphere compared to those observed by the LOGACS experiment.

REFERENCES

1. Jacchia, L. G.: Corpuscular Radiation and the Acceleration of Artificial Satellites. Nature, vol. 183, 1960, pp. 1662-1663.

2. Dessler, A. J.: Ionospheric Heating by Hydromagnetic Waves. J. Geophys. Res., vol. 64, 1959, pp. 397-401.

3. Akasofu, S.: Dynamic Morphology of Auroras. Space Science Reviews, vol. 4, 1965, pp. 498-540.

4. McIlwain, C. E.: Heating of the Lower Thermosphere by Electron Precipitation. J. Geophys. Res., vol. 65, 1960, p. 2767.

5. Cole, K. D.: Joule Heating of the Ionosphere Over Halley Bay. Nature, vol. 199, 1963, pp. 444-445.

6. Cole, K. D.: Joule Heating of the Upper Atmosphere. Australian J. Phys., vol. 15, 1962, pp. 223-235.

7. Peddington, J. H.: Mon National Astr. Soc., vol. 114, 1954, p. 114.

8. Jacchia, L. G., Verniani, F., and Slowey, J.: Geomagnetic Perturbations and Upper-Atmospheric Heating. Smithsonian Astrogeophysical Observatory Special Report, 218, 1966.

9. King-Hele, D. G.: Methods of Determining Air Density from Satellite Orbits. Ann. Geophys., vol. 22, 1966, p. 43.

10. Roemer, M.: Structure of the Thermosphere and its Variations. Ann. Geophys., vol. 25, 1969, pp. 419-437.

11. DeVries, L. L., Friday, E. W., and Jones, L. C.: Analysis of Data Deduced from Low-Altitude High Resolution Satellite Data. Space Res. VII (R. L. Smith-Rose, ed.), North Holland Publishing Company, Amsterdam, 1967, pp. 1174-1182.

12. Jacobs, R. L.: Atmospheric Density Derived from the Drag of Eleven Low-Altitude Satellites. J. Geophys. Res., vol. 72, 1967, pp. 1571-1581.

13. Lew, Stephen K.: On the Dynamics Response of the Thermosphere at Low Altitudes to Geomagnetic Disturbances. J. Geophys. Res., vol. 74, 1969, p. 5093.

REFERENCES (Concluded)

14. Foton, E. G.: LOGACS – An Orbital Accelerometer Calibration Experiment (U). TOR-0158(3110-01)-21, Aerospace Corporation, El Segundo, California, March 1968 (Confidential Report).

15. Bruce, R. W.: Upper Atmospheric Density Determined from a Low-G Accelerometer on Satellite 1967 50 B (U). TOR-0158(3110-01)-16, Aerospace Corporation, El Segundo, California, February 15, 1968 (Confidential Report).

16. Jacchia, L. G.: New Static Models of the Thermosphere and Exosphere with Empirical Temperature Profiles. Smithsonian Astrophysical Observatory Special Report, 313, 1970.

17. CIRA 1965, COSPAR International Reference Atmosphere, 1965. North Holland Publishing Company, Amsterdam, 1965.

18. Blumen, William, and Hendl, Richard G.: On the Role of Joule Heating as a Source of Gravity Wave Energy Above 100 km. J. Atmos. Sci., vol. 26, 1969, pp. 210-217.

19. Akasofu, S. I., Chapman, S., and Meng, E. I.: The Polar Electrojet. J. Atmos. and Terres. Phys., vol. 27, 1965, pp. 1275-1305.

NASA-Langley, 1971 —— 13 M175

"The aeronautical and space activities of the United States shall be conducted so as to contribute . . . to the expansion of human knowledge of phenomena in the atmosphere and space. The Administration shall provide for the widest practicable and appropriate dissemination of information concerning its activities and the results thereof."

—NATIONAL AERONAUTICS AND SPACE ACT OF 1958

NASA SCIENTIFIC AND TECHNICAL PUBLICATIONS

TECHNICAL REPORTS: Scientific and technical information considered important, complete, and a lasting contribution to existing knowledge.

TECHNICAL NOTES: Information less broad in scope but nevertheless of importance as a contribution to existing knowledge.

TECHNICAL MEMORANDUMS: Information receiving limited distribution because of preliminary data, security classification, or other reasons.

CONTRACTOR REPORTS: Scientific and technical information generated under a NASA contract or grant and considered an important contribution to existing knowledge.

TECHNICAL TRANSLATIONS: Information published in a foreign language considered to merit NASA distribution in English.

SPECIAL PUBLICATIONS: Information derived from or of value to NASA activities. Publications include conference proceedings, monographs, data compilations, handbooks, sourcebooks, and special bibliographies.

TECHNOLOGY UTILIZATION PUBLICATIONS: Information on technology used by NASA that may be of particular interest in commercial and other non-aerospace applications. Publications include Tech Briefs, Technology Utilization Reports and Technology Surveys.

Details on the availability of these publications may be obtained from:

SCIENTIFIC AND TECHNICAL INFORMATION OFFICE

NATIONAL AERONAUTICS AND SPACE ADMINISTRATION

Washington, D.C. 20546